Hindawi Publishing Corporation
International Journal of Antennas and Propagation
Volume 2008, Article ID 410786, 7 pages
doi:10.1155/2008/410786

Research Article

UWB Directive Triangular Patch Antenna

A. C. Lepage,[1] X. Begaud,[1] G. Le Ray,[2] and A. Sharaiha[2]

[1] *GET/Télécom Paris, CNRS UMR 5141, 46 rue Barrault, 75634 Paris Cedex 13, France*
[2] *IETR, CNRS UMR 6164, Université de Rennes 1, Groupe Antennes et Hyperfréquences, Bâtiment 11D, 35042 Rennes Cedex, France*

Correspondence should be addressed to A. C. Lepage, anne-claire.lepage@enst.fr

Received 1 May 2007; Accepted 21 October 2007

Recommended by Dejan Filipovic

Compact directive UWB antennas are presented in this paper. We propose an optimization of the F-probe fed triangular patch antenna. The new design achieves an impedance bandwidth of 69% (3–6.15 GHz) and presents good radiation characteristics over the whole impedance bandwidth. The average gain is 6.1 dB. A time-domain study has been performed to characterize the antenna behavior in case a UWB pulse is used. Finally, we propose an alternative solution to facilitate the manufacturing process using metallized foam technology. It also improves the robustness of the antenna as well as reducing its cost.

1. INTRODUCTION

One of the key issues of the emerging ultra-wide band (UWB) technology is the design of low cost compact antennas.

Many researches are focused on omnidirectional antennas because their wide beamwidth enables to communicate with radio elements whatever their position is.

But directional antennas also present some interest. In fact, on the transmitter side, even if regulation authorities have limited the effective isotropic-radiated power (EIRP), the use of directional antennas enables to reduce radiation in undesired directions and thus improves power consumption. On the receiver side, the antenna gain adds a few and precious dB in the link budget.

Concerning the applications, directional antennas could be placed on a wall or implemented in a sectorized radio topology (radio-access point) or in a terminal using multiple directive antennas (antenna diversity). It is also possible for some specific applications that the user points the antenna in the desired direction, for example, for a fast download between his terminal and a PC.

With their low thickness, conformability, compactness and low cost, microstrip antennas are very attractive for such applications, but they suffer from their inherently narrow bandwidth. In order to solve this problem, a well-known technique consists in using low permittivity and thick substrate.

The extreme case is using the air as the substrate. This solution will maximize the size of the structure. However, it remains attractive for some applications as the antenna is still compact.

It has been demonstrated in [1] that increasing the thickness of the substrate induces an inductive effect on input impedance which can be offset by adding a capacitance to obtain a wide-band behavior.

Thus, the L-shaped probe proposed in [2] to feed the patch by electromagnetic coupling enables to widen the bandwidth. A triangular patch fed by an L-shaped probe achieves 42% impedance bandwidth and a maximum gain of 6 dBi [3]. An F-shaped probe rectangular patch antenna with an impedance bandwidth of 64% has also been designed in [4] but the radiation pattern was not stable over the bandwidth due to the excitation of successive radiating modes of the patch.

In [5], we have proposed a triangular patch fed by an F-shaped probe. This new structure has stable radiation pattern over the impedance bandwidth of 47%, from 3.1 to 5 GHz.

In this paper, we present an improvement of this antenna with a wider bandwidth.

We also propose an alternative solution to manufacture the probe and the patch using metallized foam technology in order to improve its reproducibility and reduce its cost.

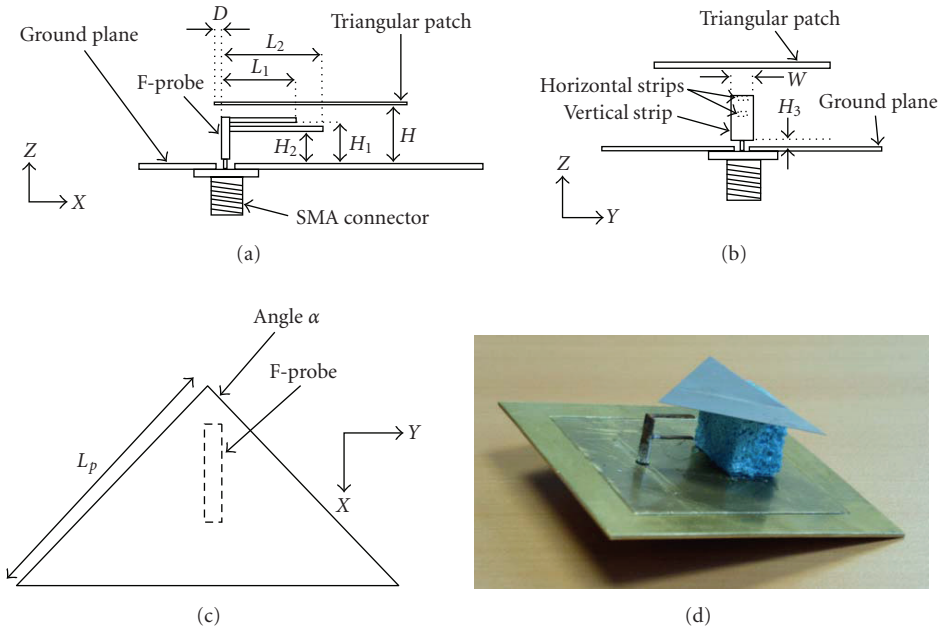

Figure 1: Geometry of the antenna and prototype.

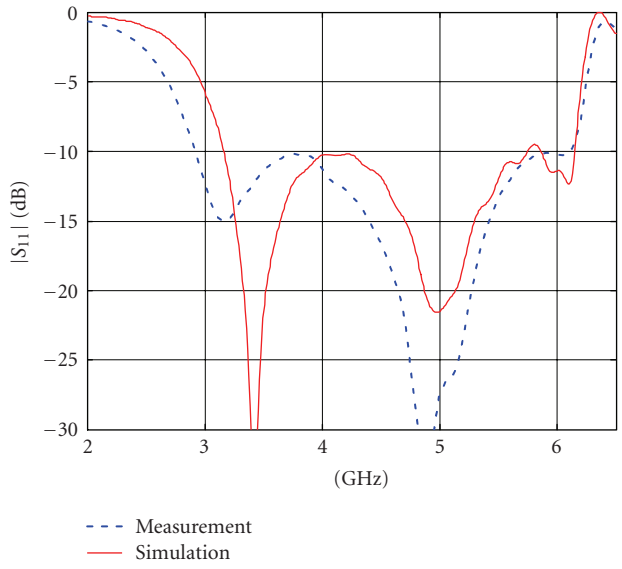

Figure 2: Measured and simulated reflection coefficient magnitude $|S_{11}|$ versus frequency.

2. DESCRIPTION OF THE F-PROBE ANTENNA

The geometry of the antenna is presented in Figure 1. The F-probe is made of a bended 0.2 mm thick metallic rectangular strip on which a second strip has been welded. The whole is welded to an SMA connector whose central conductor goes through the square ground plane.

The radiating element is an isosceles triangle cut out of a steel sheet which is electromagnetically fed by the F-probe. The triangular shape has been chosen because it has been demonstrated in [6] that three of the five first modes (TM_{10}, TM_{20}, and TM_{21}) present similar radiation pattern, polarization, and input impedance. The triangle is centered above the ground plane and supported by a foam layer; it has been verified to have a permittivity close to the air.

Dimensions of the structure are as follows: $L_p = 36$ mm, $D = 0.6$ mm, $H_3 = 0.4$ mm, $\alpha = 84°$, $H = 14.9$ mm, $H_1 = 10.05$ mm, $H_2 = 5.6$ mm, $L_1 = 9.9$ mm, $L_2 = 10.8$ mm, $w = 3.6$ mm, horizontal strips width = 1.2 mm, ground plane size = 67×67 mm, probe thickness = 0.4 mm.

The antenna has been simulated with CST Microwave Studio software.

This optimized structure is the result of a parametric study which has demonstrated that it is possible to generate multiple resonances close to each other when the lengths of the horizontal strips of the probe are slightly different.

However, a capacitance effect caused mismatching. That is why we added an inductive effect on the probe by increasing the width of the vertical strip. Finally, the optimization has also been done on H, H_1, and H_2 to obtain a good impedance matching.

This new probe is different from the one presented in [5] whose strips had all the same width and very different lengths.

At the beginning of the study, the angle α value was 90°. But due to constraints concerning the length of the base of the triangle, the value of α has been reduced to 84°.

3. RESULTS AND ANALYSIS

3.1. Frequency-domain results

The simulated and measured return loss is presented in Figure 2. The measured bandwidth, defined for a reflection coefficient $|S_{11}|$ lower than −10 dB, reaches 69%

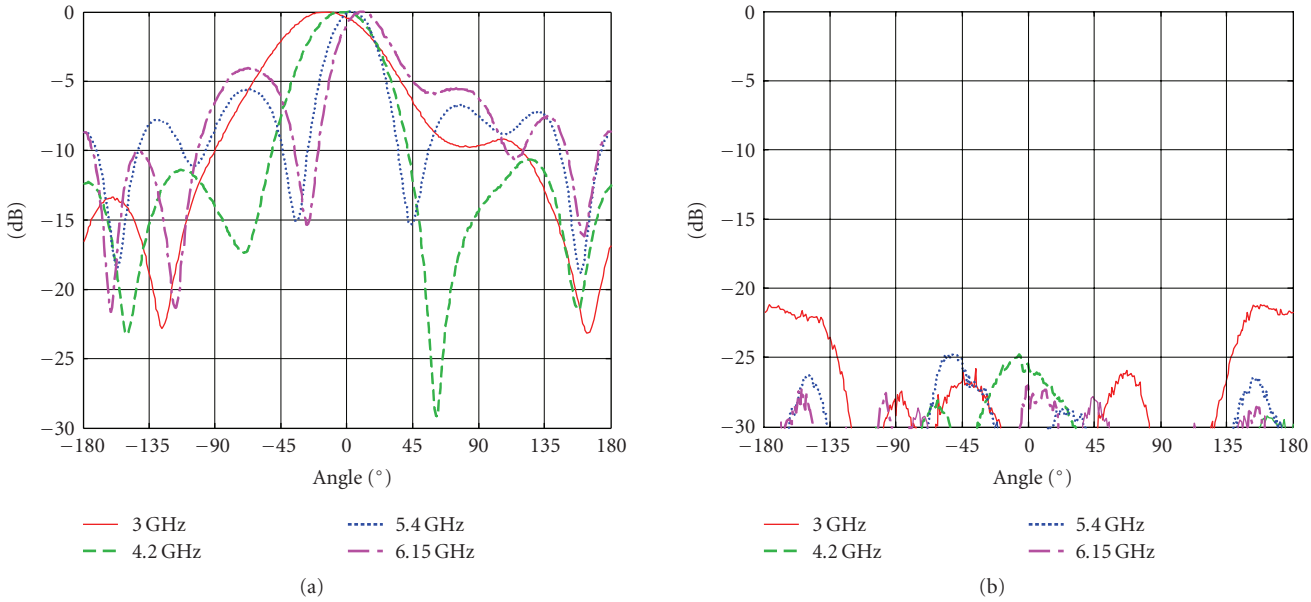

Figure 3: Radiation pattern in the E-plane.

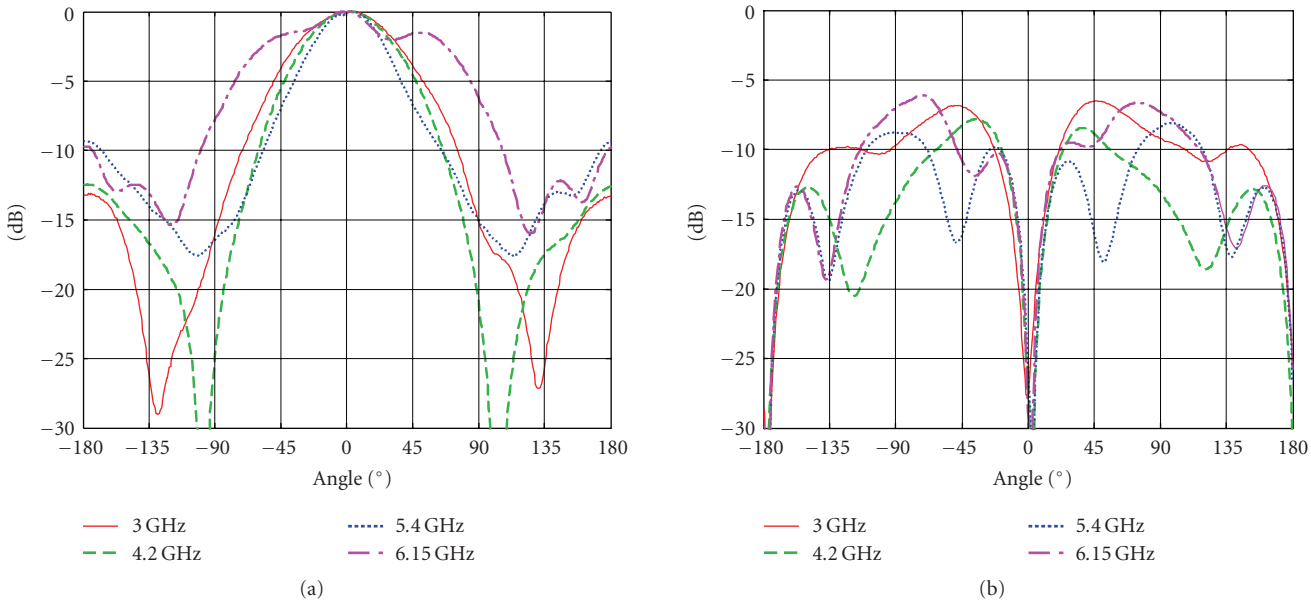

Figure 4: Radiation pattern in the H-plane.

(3.01–6.15 GHz). Good agreement between simulation and measurement is observed. And it has been demonstrated that the ground plane size has no influence on impedance matching. Figure 3 presents measured radiation pattern at different frequencies over the bandwidth in the E-plane (XZ plane) and Figure 4 in the H-plane (YZ plane).

Main lobe direction remains very stable in the H-plane and quite stable in the E-plane with a maximum variation of 15 degrees.

Cross-polarization level is very low in the E-plane and in the main lobe direction of the H-plane. In the H-plane, it is maximum (−6.7 dB) outside the main lobe for $\theta = \pm 82^\circ$ at 6.15 GHz.

Measured and simulated gains in the main lobe direction are presented in Figure 5.

Measured gain is quite stable up to 5.5 GHz and decreases at higher frequencies. Average measured gain is 6.1 dB.

Good agreement between simulation and measurement is observed except for highest frequencies, which requires new measurements.

The ground plane size influence on gain has also been studied.

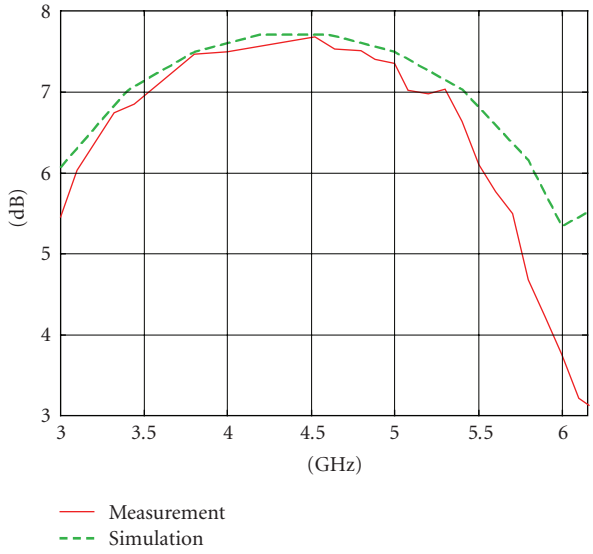

Figure 5: Comparison between simulated and measured gain in the main lobe direction over the bandwidth.

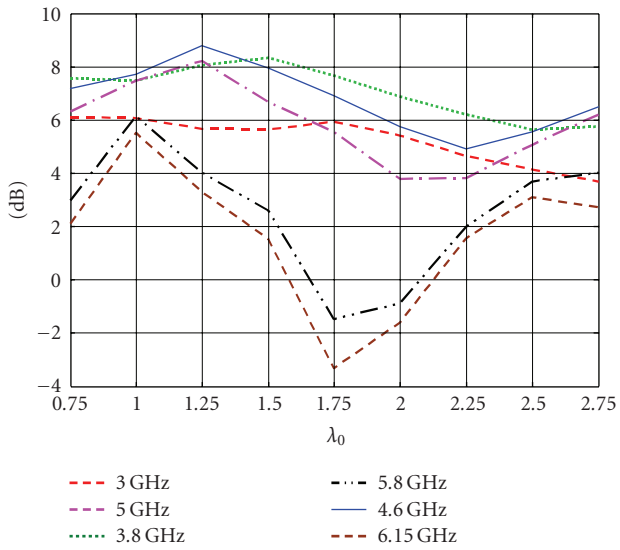

Figure 6: Gain in the main lobe direction as a function of the ground plane size at different frequencies. (λ_0 is the wavelength corresponding to the central frequency of the impedance bandwidth of the antenna).

Figure 6 presents the gain in the main lobe direction ($\theta = 0°$, $\varphi = 0°$) as a function of the ground plane size at different frequencies. It can be deduced that a ground plane size of λ_0 by λ_0 gives the smallest variation of the gain and the best average value over the bandwidth (λ_0 is the wavelength at $f = 4.58$ GHz). That is why we chose this size for the prototype.

3.2. UWB specific time- and frequency-domain analyses

Evaluation of input impedance, radiation pattern, and gain as a function of frequency is not sufficient in case of using time-domain modulation schemes, for example, pulse position modulation. The distortion of the pulse resulting from the dispersive nature of the antenna has also to be analyzed.

For this purpose, we measured the transfer function as a function of the angular coordinates using a reference antenna as described in [7].

Once it is determined, it is possible to calculate the radiated field.

We chose a Gaussian excitation impulse whose spectrum is presented in Figure 7. Figure 8 presents the excitation signal and the measured and simulated radiating field in the main lobe direction.

From Figure 8, we can observe very good agreement between simulation with CST Microwave Studio and the measurement. Although we remark some distortion, it seems to be moderate: the radiated pulse is not very different from the

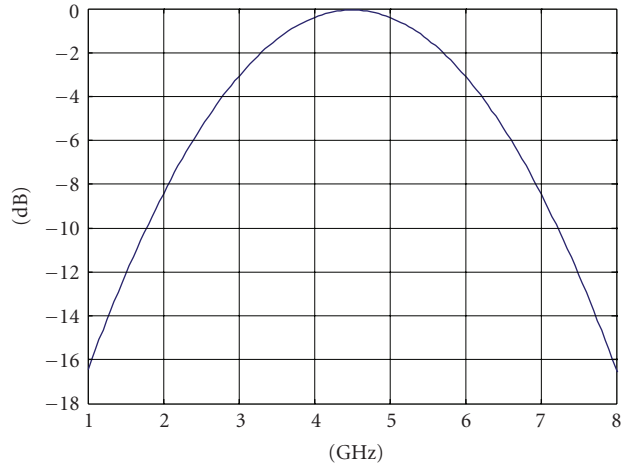

Figure 7: Spectrum of the excitation signal.

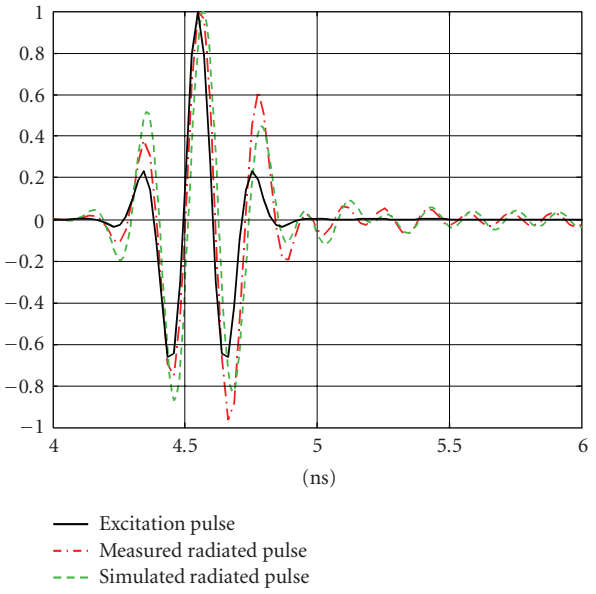

Figure 8: Excitation signal and radiated field in the main lobe direction.

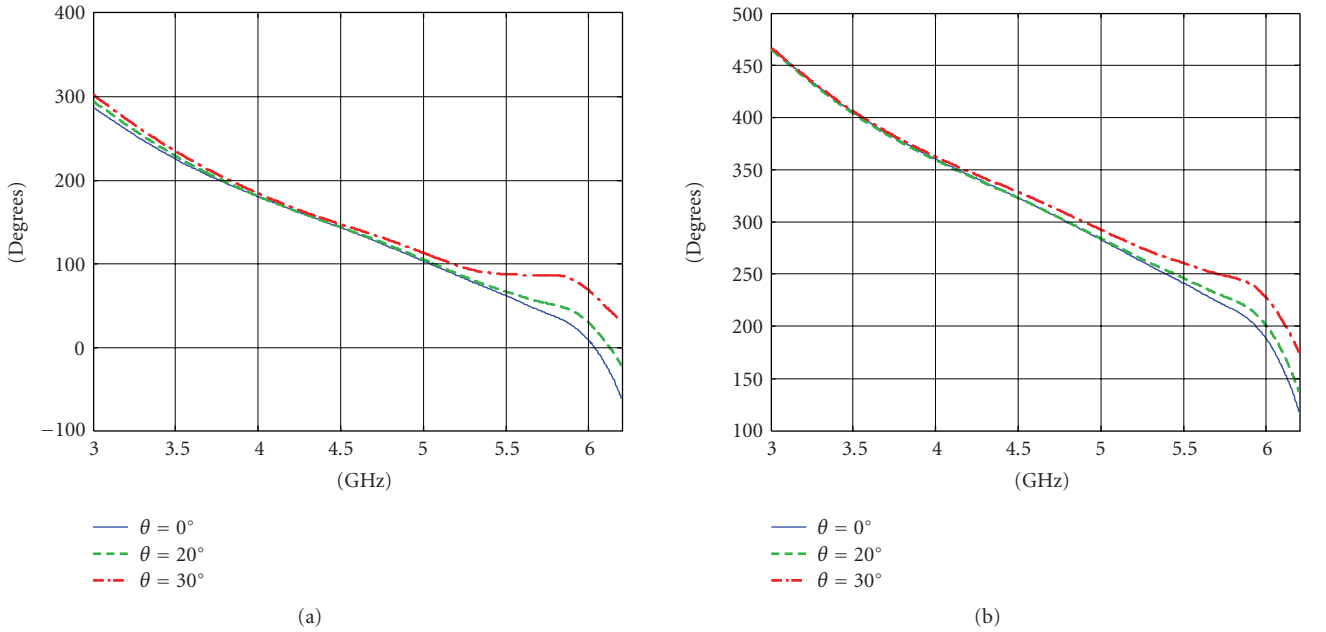

Figure 9: Simulated phase of the far-field (copolarization) in the E-plane (left) and in the H-plane at different angles in the main lobe.

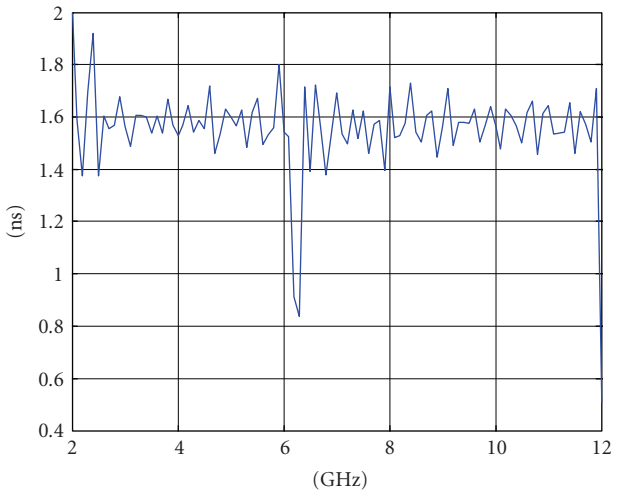

Figure 10: Group delay in the main lobe direction $\theta = 0°$ between 2 and 12 GHz.

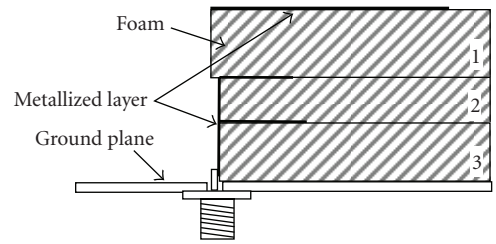

Figure 11: Structure of the antenna using metallized foam technology.

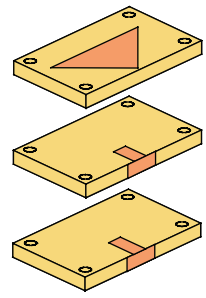

Figure 12: Metallized foam blocks before assembly.

excitation signal. It is a bit larger due to the fact that the antenna has filtered all frequencies outside its impedance bandwidth.

Figure 9 shows the evolution of the far-field phase (copolarization component) over the bandwidth for different values of elevation angle in the main lobe in the E- and H-planes. It is nearly linear which confirms low pulse distortion.

In order to quantify the phase linearity, we studied the group delay τ_g, defined in [8] as: $\tau_g = -(\partial\varphi/2\pi\partial f)$, where φ is the phase and f the frequency.

And the standard deviation of the group delay defined in [8] as $\sigma_{\text{gd}} = \sqrt{(1/\Delta f)\int_{f_1}^{f_2}(\tau_{\text{g}} - \overline{\tau_g})^2 df}$, where f_1 and f_2 are the boundaries of the impedance bandwidth Δf and $\overline{\tau_g}$ is the average group delay.

For the F-probe antenna, the standard deviation is under 250 ps over the beamwidth.

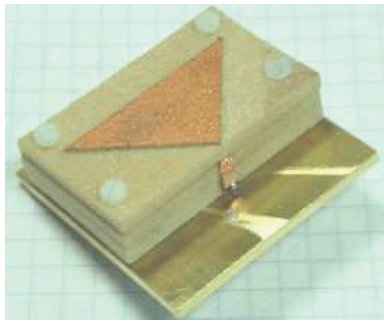

Figure 13: Triangular patch F-probe antenna using metallized foam technology.

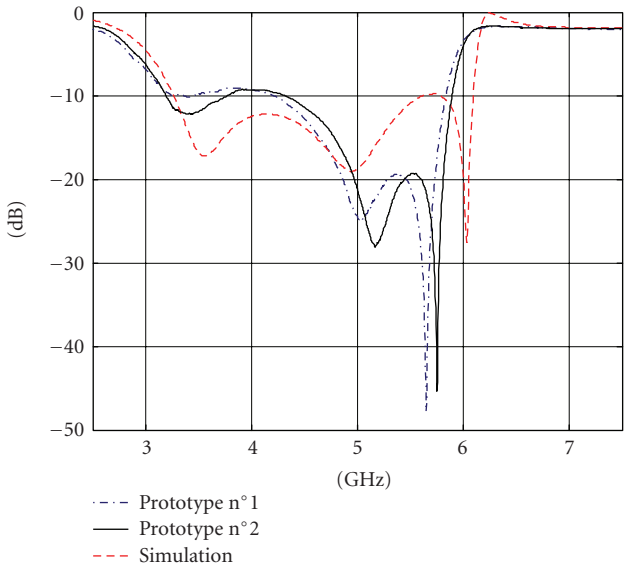

Figure 14: Measured and simulated reflection coefficient magnitude $|S_{11}|$ versus frequency.

4. F-PROBE ANTENNAS USING METALLIZED FOAM TECHNOLOGY

The F-probe triangular patch antenna presents interesting features. But one critical issue still persists: the difficulty of realization which is directly linked to the cost. In fact, the manufacturing of the F-probe is a real technological issue, especially the welding of the lower horizontal strip to the bended strip. Moreover, the robustness of the antenna has to be improved.

We retained an innovative solution developed at IETR (Institut d'Electronique et des Télécommunications de Rennes) which enables to metallize low-permittivity foam of arbitrary geometry [9].

Thus, we realized the antenna with a quite rigid foam whose electrical permittivity is 1.23.

Due to this new permittivity value, it has been necessary to resize the antenna. New dimensions are as follows: L_p = 32.5 mm, D = 0.6 mm, $\alpha = 84°$, H = 13.9 mm, H_1 = 9.7 mm, H_2 = 5.3 mm, L_1 = 9.1 mm, L_2 = 9.9 mm, w = 3.25 mm, horizontal strips width = 1.1 mm, ground plane size = 54 × 54 mm, metallization thickness = 0.02 mm.

The radiating patch and the F-probe are metallized on 3 different blocks of foam. (Figures 11 and 12): the triangle is metallized on the block n°1, the upper vertical part of the probe and the upper horizontal strip are on the block n°2 and the lower vertical part and the lower strip are metallized on the block n°3. As before, the ground plane is cut in a brass sheet. The SMA connector is welded to the vertical metallized part directly on the foam. The three blocks are screwed together and also to the ground plane with 4 nylon screws. (Figure 13).

In order to evaluate the reproducibility of the process, we realized two prototypes.

Figure 14 presents the measurement of the magnitude of the reflection coefficient for the two prototypes and the comparison with the simulation result.

First of all, results are similar for the two prototypes which demonstrate the good reproducibility of the manufacturing process.

The measured bandwidth reaches 58% (3.2–5.8 GHz).

The agreement between measurement and simulation is satisfying.

Due to space constraints, radiation patterns are not shown but they appear to be similar to those presented in Section 3.

Since the relative electric permittivity is 1.23, the gain value is similar to the one of the previous design.

The next step of improvement of the manufacturing of this antenna will be the metallization of the ground plane.

5. CONCLUSION

In this article, we have presented an optimization performed on the F-probe triangular patch antenna. The new design achieves an impedance bandwidth of 69% with a stable radiation pattern over the bandwidth and is quite compact ($\lambda_0 \times \lambda_0 \times 0.22\,\lambda_0$). A time domain study has also shown that the antenna distorts the excitation pulse in a moderate way.

A solution has also been proposed for an easier realization and a better robustness of the probe in the purpose of minimizing manufacturing costs and improving reproducibility.

At this time, this antenna is integrated in an industrial UWB test platform.

ACKNOWLEDGMENT

This work has been done in collaboration with the UEI-AAR laboratory of ENSTA, Paris, France.

REFERENCES

[1] D. H. Schaubert, D. M. Pozar, and A. Andrew, "Effect of microstrip antenna substrate thickness and permittivity: comparison of theories with experiment," *IEEE Transactions on Antennas and Propagation*, vol. 37, no. 6, pp. 677–682, 1989.

[2] K. M. Luk, C. L. Mak, Y. L. Chow, and K. F. Lee, "Broadband microstrip patch antenna," *Electronics Letters*, vol. 34, no. 15, pp. 1442–1443, 1998.

[3] C. L. Mak, K. M. Luk, and K. F. Lee, "Wideband triangular patch antenna," *IEE Proceedings: Microwaves, Antennas and Propagation*, vol. 146, no. 2, pp. 167–168, 1999.
[4] B. L. Ooi, C. L. Lee, and P. S. Kooi, "A novel F-probe-fed broadband patch antenna," *Microwave and Optical Technology Letters*, vol. 30, no. 5, pp. 355–356, 2001.
[5] A. C. Lepage and X. Begaud, "A compact ultrawideband triangular patch antenna," *Microwave and Optical Technology Letters*, vol. 40, no. 4, pp. 287–289, 2004.
[6] K. F. Lee, K. M. Luk, and J. S. Dahele, "Characteristics of the equilateral triangular patch antenna," *IEEE Transactions on Antennas and Propagation*, vol. 36, no. 11, pp. 1510–1518, 1988.
[7] H. Ghannoum, *Etude conjointe antenne/canal pour les communications ultra Large Bande en présence du corps humain*, Ph.D. thesis, ENST, Paris, France, 2006.
[8] C. Roblin, S. Bories, and A. Sibille, "Characterization tools in the time domain," in *Proceedings of International Workshop on Ultra Wideband Systems (IWUWBS '03)*, Oulu, Finland, June 2003.
[9] S. Chainon and M. Himdi, "2D and 3D metallized foam technology applied to conformal antennas," in *Proceedings of the 3rd Workshop on Conformal Antennas*, Bonn, Germany, October 2003.